Comparison of Filtering Options For Ballistic Coefficient Estimation

Robert Jesionowski*
Sparta Inc., Arlington, VA 22209
and
Paul Zarchan **
The Charles Stark Draper Laboratory, Inc., Cambridge, MA 02139

Abstract

The capabilities of a linear decoupled Kalman filter and two extended Kalman filters were examined when tracking an object as it enters the atmosphere. The filters were given identical radar range and elevation data. The first extended filter estimates the position, velocity, and inverse ballistic coefficient; the second estimates position, velocity and the ballistic coefficient. The linear filter estimates position, velocity and acceleration and derives the ballistic coefficient from those estimates. The paper will show that the performance of the linear filter is inferior to that of the extended filters, while the performances of the extended filters are nearly identical.

Introduction

An accurate estimation of a tactical ballistic missile's ballistic coefficient is important for the guidance system of a pursuing interceptor, and for the launch logic used to place the interceptor on a collision triangle. The ballistic coefficient estimate is used both for the prediction of the expected intercept point, and for acceleration estimates in predictive guidance laws. Inaccurate estimates of a target's ballistic coefficient can cause the interceptor to waste a great deal of acceleration to compensate for intercept point prediction error. Inaccuracies in the estimate of the ballistic coefficient may also lead to missile acceleration saturation because the interceptor will be chasing an apparent target maneuver.

Three different filters are compared in this study. The first is a six-state, linear Kalman filter ($\bar{r}$, $\bar{v}$, $\bar{a}$). The other two are five-state extended Kalman filters ($\bar{r}$, $\bar{v}$, $\frac{1}{\beta}$), ($\bar{r}$, $\bar{v}$, β). Three cases will be examined: a constant ballistic coefficient case, a case with the ballistic coefficient decreasing linearly with time, and a case with the ballistic coefficient changing step-wise with time. The error in the estimate of the ballistic coefficient will be the sole measure of performance.

The only external forces acting upon the body will be drag and flat earth gravity; the drag force is driven by the ballistic coefficient. Hence, the motion of the body is restricted to a plane.

The paper will show that the extended filters outperform the linear filter in every case examined. This difference is due to the nature of the endo-atmospheric dynamics. It will be shown that, despite the differences in the two extended filters, they yield similar results. It appears that the error in the estimate of β is a function of the plant dynamics only. Varying the states of the algorithm estimating a non-linear system does not affect performance in this example.

Filter Overview

The three filter designs are described in this section. The first is a linear decoupled filter which estimates position, velocity, and acceleration. The estimated ballistic coefficient is computed using the state estimates. The first extended filter uses position and velocity in each direction, and the inverse ballistic coefficient, α. The second extended filter also estimates position and velocity, but it estimates the ballistic coefficient β directly instead of α.

For all three filters the propagation of the state covariance is done with the following[1]:

$$\bar{\mathbf{P}}_{\mathbf{k+1}} = \mathbf{\Phi}(\mathbf{t_{k+1}}, \mathbf{t_k})\hat{\mathbf{P}}_{\mathbf{k}}\mathbf{\Phi}^{\mathbf{T}}(\mathbf{t_{k+1}}, \mathbf{t_k}) + \mathbf{Q_k}. \quad (1)$$

where $\bar{\mathbf{P}}_{k+1}$ is the propagated state covariance, $\hat{\mathbf{P}}_k$ is the last updated state covariance, $\Phi(t_{k+1}, t_k)$ is the state transition matrix, and $\mathbf{Q}_k$ is the plant noise. The

*Principal Engineer, Systems Analysis Division, Member AIAA

**Principal Member of Technical Staff, Associate Fellow AIAA

particulars of the state transition matrices and plant noise vary from filter to filter.

For all three filters, the update equations for state and state covariance are:

$$\hat{\mathbf{x}}_{\mathbf{k+1}} = \bar{\mathbf{x}} + \mathbf{K}\,(\,\hat{\mathbf{z}}_{\mathbf{k+1}} - \mathbf{H}\,\bar{\mathbf{x}}_{\mathbf{k+1}}\,) \quad (2)$$

$$\hat{\mathbf{P}}_{\mathbf{k+1}} = (\mathbf{I} - \mathbf{KH})\bar{\mathbf{P}}_{\mathbf{k+1}}(\mathbf{I} - \mathbf{KH})^{\mathbf{T}} + \mathbf{KRK}^{\mathbf{T}}, \quad (3)$$

and the equation for the Kalman gain are:

$$\mathbf{K} = \bar{\mathbf{P}}\,\mathbf{H}^{\mathbf{T}}[\mathbf{H}\,\bar{\mathbf{P}}\,\mathbf{H}^{\mathbf{T}} + \mathbf{R}]^{-1}. \quad (4)$$

The measurement is the position as measured by the radar,

$$\hat{\mathbf{z}}_{\mathbf{k+1}} = \mathbf{H}\,\mathbf{x}_{\mathbf{k}} + \nu_{\mathbf{k}}, \quad (5)$$

where $\hat{\mathbf{z}}_{k+1}$ is the latest measurement, $\mathbf{x}_k$ is the true position of the object, $\mathbf{H}$ is the matrix relating the measurement to the state where:

$$\mathbf{H} = \begin{bmatrix} 1 & 0 & 0 & 0 & 0 & 0 \\ 0 & 1 & 0 & 0 & 0 & 0 \end{bmatrix}, \quad (6)$$

and ν_k is the measurement noise.

Linear Decoupled Filter

The linear decoupled Kalman filter has been used in many fielded systems. The filter gains for the linear decoupled Kalman filter can be computed independently of the state estimate. The state equation upon which the filter is based is given by

$$\begin{bmatrix} \dot{x} \\ \dot{y} \\ \ddot{x} \\ \ddot{y} \\ \dddot{x} \\ \dddot{y} \end{bmatrix} = \begin{bmatrix} 0 & 0 & 1 & 0 & 0 & 0 \\ 0 & 0 & 0 & 1 & 0 & 0 \\ 0 & 0 & 0 & 0 & 1 & 0 \\ 0 & 0 & 0 & 0 & 0 & 1 \\ 0 & 0 & 0 & 0 & 0 & 0 \\ 0 & 0 & 0 & 0 & 0 & 0 \end{bmatrix} \begin{bmatrix} x \\ y \\ \dot{x} \\ \dot{y} \\ \ddot{x} \\ \ddot{y} \end{bmatrix} + \begin{bmatrix} 0 \\ 0 \\ 0 \\ 0 \\ \omega \\ \omega \end{bmatrix} + \begin{bmatrix} 0 \\ 0 \\ 0 \\ -g_e \\ 0 \\ 0 \end{bmatrix} \quad (7)$$

where ω is white noise represents the predicted jerk or agility in the dynamics, and g_e is the flat earth gravity term. The states are decoupled, therefore each dimension is independent of the others. The position, velocity, and acceleration are then assumed to be subject to the following discrete-time dynamics, propagating from the current time t_k to t_{k+1}:

$$\mathbf{\Phi}(t_{k+1}, t_k) \equiv \begin{bmatrix} \mathbf{I} & \Delta t\mathbf{I} & \frac{1}{2}\Delta t^2\mathbf{I} \\ 0 & \mathbf{I} & \Delta t\mathbf{I} \\ 0 & 0 & \mathbf{I} \end{bmatrix}, \quad (8)$$

where $\mathbf{I} = \begin{bmatrix} 1 & 0 \\ 0 & 1 \end{bmatrix}$ and: $\Delta t = t_{k+1} - t_k$.

Therefore the propagation of the state becomes:

$$\bar{\mathbf{x}}_{\mathbf{k+1}} = \mathbf{\Phi}(\mathbf{t_{k+1}}, \mathbf{t_k})\,\hat{\mathbf{x}}_{\mathbf{k}} + \mathbf{G_k u_k} \quad (9)$$

where $\bar{\mathbf{x}}_{k+1}$ is the propagated state estimate, $\hat{\mathbf{x}}_k$ is the estimated state at the time of the last update. The second term, $\mathbf{G_k u_k}$, is added to the state propagation as a means of treating the acceleration due to gravity as a bias. This was done in order to improve the performance of the linear filter. This bias term is defined as:

$$\mathbf{G_k u_k} = \begin{bmatrix} 0 \\ \frac{1}{2}\Delta t^2 \\ 0 \\ \Delta t \\ 0 \\ 0 \end{bmatrix} [-g_e] \quad (10)$$

The measurement noise is zero mean and Gaussian where

$$\mathbf{E}[\nu] = \mathbf{0} \quad (11)$$

and

$$\mathbf{R} = \mathbf{E}[\,\nu\,\nu^{\mathbf{T}}]. \quad (12)$$

For the linear filter, the measurement covariance is:

$$\mathbf{R} = \begin{bmatrix} {\sigma_r}^2 cos^2\theta + R^2 sin^2\theta {\sigma_\theta}^2 & 0 \\ 0 & {\sigma_r}^2 sin^2\theta + R^2 cos^2\theta {\sigma^2}_\theta \end{bmatrix}, \quad (13)$$

and R is the range from the radar to the target, θ is the elevation angle to the target, and σ_a is the angular error in the measurement, and σ_r is the range error in the measurment.

The plant noise covariance matrix, $\mathbf{Q}$, is a function of ω, the uncertainty in the dynamics equations. ω is assumed to be zero mean and Gaussian therefore:

$$\mathbf{E}[\omega] = \mathbf{0} \quad (14)$$

and

$$\mathbf{Q} = \mathbf{E}[\,\omega\,\omega^{\mathbf{T}}]. \quad (15)$$

The process noise for the linear filter assumes a white noise jerk model. The resulting plant noise covariance is:

$$\mathbf{Q} = \begin{bmatrix} \frac{\Delta t^5}{20}\mathbf{I} & \frac{\Delta t^4}{8}\mathbf{I} & \frac{\Delta t^3}{6}\mathbf{I} \\ \frac{\Delta t^4}{8}\mathbf{I} & \frac{\Delta t^3}{3}\mathbf{I} & \frac{\Delta t^2}{2}\mathbf{I} \\ \frac{\Delta t^3}{6}\mathbf{I} & \frac{\Delta t^2}{2}\mathbf{I} & \Delta t\mathbf{I} \end{bmatrix} \epsilon^2 \quad (16)$$

where ϵ is predicted error in the constant acceleration assumption[2]. In the cases studied we are assuming ϵ is $(5\ g_e)^2/\Delta t_{tot}$ where g_e is flat earth gravity and Δt_{tot} is the total expected simulation time.

Figure 1 shows the acceleration history of a body with constant ballistic coefficient as it enters the atmosphere. The value for ϵ used in the study is based upon the average number of g's pulled during the object entry into the atmosphere, or approximately 5g's.

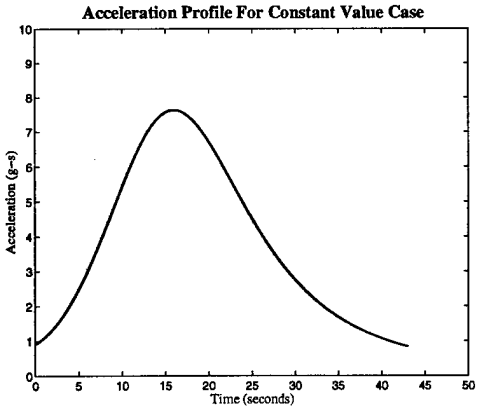

Figure 1: Acceleration History for Constant β

In order to back out β from the estimated state one needs to start with the definition of the ballistic coefficient:

$$\beta = \frac{S\,C_d}{m} \tag{17}$$

where S is the area of the body, C_d is the coefficient of drag of the body, and m is the mass of the body. Recalling that, $\bar{\mathbf{a}}$, the acceleration, acting upon the body is assumed to be only the sum of the accelerations due to drag and gravity:

$$\bar{\mathbf{a}} \;=\; \frac{\bar{\mathbf{D}}}{m} \;+\; \bar{\mathbf{g}}. \tag{18}$$

taking the definition of the drag force and gravitational acceleration and expanding them out in Eq.(17) yields:

$$\bar{\mathbf{a}} \;=\; -\frac{1}{2}\,\rho V^2\,\frac{S\,C_d}{m}\,\hat{\mathbf{v}} \;+\; \begin{bmatrix} 0 \\ -g_e \end{bmatrix} \tag{19}$$

where $-\hat{\mathbf{v}}$ is the drag direction, g_e is the flat earth gravity, V is object speed and ρ is the exponential atmospheric density where:

$$\rho \;=\; c_1 e^{\frac{y}{c_2}} \tag{20}$$

Eq.(18) can in turn be rewritten as:

$$\bar{\mathbf{d}} \;=\; -\frac{q}{\beta}\,\hat{\mathbf{v}} \quad \text{where} \quad \bar{\mathbf{d}} = \begin{bmatrix} \ddot{x} \\ \ddot{y} + g_e \end{bmatrix} \tag{21}$$

where q is the dynamic pressure. Taking the vector magnitude of each side of the equation and solving for the ballistic coefficient yields:

$$\beta = \frac{q}{\sqrt{\ddot{x}^2 + (\ddot{y} + g_e)^2}} \tag{22}$$

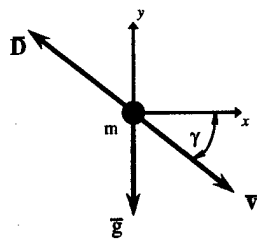

Figure 2: Free Body Diagram for Extended Filter Dynamics

Extended Kalman Filters

The two extended filters used in this study each have five states. The states of the the first filter and the corresponding differential equations governing them, based upon the dynamics shown in the free body diagram in Figure 2, are as follows:

$$\mathbf{x} = \begin{bmatrix} x \\ y \\ \dot{x} \\ \dot{y} \\ \alpha \end{bmatrix} \quad \text{and} \quad \dot{\mathbf{x}} = \begin{bmatrix} \dot{x} \\ \dot{y} \\ \alpha\, q\, cos\gamma \\ g_e \,-\, \alpha\, q\, sin\gamma \\ w \end{bmatrix}, \tag{23}$$

where γ is the flight path angle, and α is the inverse ballistic coefficient.

For the second filter the states and differential equations are:

$$\mathbf{x} = \begin{bmatrix} x \\ y \\ \dot{x} \\ \dot{y} \\ \beta \end{bmatrix} \quad \text{and} \quad \dot{\mathbf{x}} = \begin{bmatrix} \dot{x} \\ \dot{y} \\ \frac{q\,cos\gamma}{\beta} \\ g_e \,-\, \frac{q\,sin\gamma}{\beta} \\ w \end{bmatrix}. \tag{24}$$

For both extended filters, the computation of the state transition matrices, $\mathbf{\Phi}(t_{k+1}, t_k)$, is done by computing the partial derivatives of the state via a central difference method:

$$\mathbf{\Phi}(t_{k+1}, t_k) \;=\; \frac{\partial \mathbf{x}(t_{k+1})}{\partial \mathbf{x}(t_k)}. \tag{25}$$

Unlike the linear filter, Φ is only used in the solution to the Ricatti equation, Eq.(1), to propagate the state covariance. The state itself is propagated using the differential equations in Eq.(22) and Eq.(23).

For both extended filters, the measurement covariance is:

$$\mathbf{R} = \begin{bmatrix} \sigma_r{}^2 cos^2\theta + R^2 sin^2\theta \sigma_\theta{}^2 & (\sigma_r{}^2 - R^2\sigma_\theta{}^2) sin\theta cos\theta \\ (\sigma_r{}^2 - R^2\sigma_\theta{}^2) sin\theta cos\theta & \sigma_r{}^2 sin^2\theta + R^2 cos^2\theta \sigma^2{}_\theta \end{bmatrix}, \tag{26}$$

The plant noise covariance $\mathbf{Q}$ has the following form:

$$\mathbf{Q} = \begin{bmatrix} \frac{\eta^2\Delta t^4}{4}\mathbf{I} & \frac{\eta^2\Delta t^3}{2}\mathbf{I} & 0 \\ \frac{\eta^2\Delta t^3}{2}\mathbf{I} & \eta^2\Delta t^2\mathbf{I} & 0 \\ 0\,0 & 0\,0 & \kappa\Delta t \end{bmatrix}, \quad (27)$$

where κ is the predicted error due the constant ballistic coefficient assumption. The corresponding plant noise, η, applied to the position and velocity components of the plant noise covariance, is based upon a piecewise-constant-acceleration-model assumption[2].

For the first extended filter, the predicted error due to the ballistic coefficient was computed using

$$\kappa = \frac{(\frac{1}{\beta} - \frac{1}{\hat{\beta}_0})^2}{\Delta t_{tot}} = \frac{(\alpha - \hat{\alpha}_0)^2}{\Delta t_{tot}}, \quad (28)$$

where β is the true ballistic coefficient and $\hat{\beta}_0$ is the initial estimate of the true ballistic coefficient.

Similarly, for the second extended filter the predicted error due to the ballistic coefficient was computed using

$$\kappa = \frac{(\beta - \hat{\beta}_0)^2}{\Delta t_{tot}}. \quad (29)$$

The true β for the cases run was approximately 2500 kg/m^2, and the initial estimate was 4000 kg/m^2. The predicted total run-time of the simulation, Δt_{tot}, was set at 40 seconds.

Results

For all three cases, the body starts at an altitude of 30.48km (100 kft) with a speed of 1.8288 km/s (6000 ft/s) at a flight path angle of 45^o. The atmospheric density constants, c_1 and c_2 from Eq.(18), are 1.7523 kg/m^3 and 6705.6 m respectively. For completeness, Figure 3 shows the trajectory used for the constant β profile case.

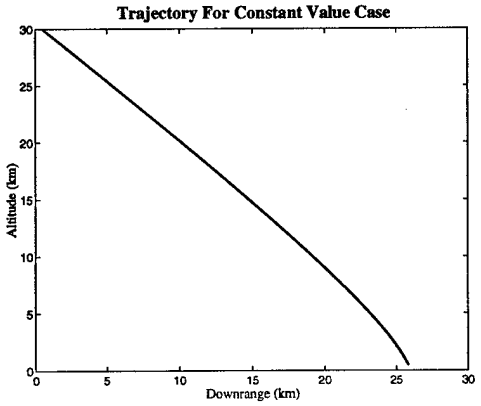

Figure 3: Trajectory for Constant β Profile

The sensor is located at sea-level, 27km downrange from the trajectory starting point. The sensor angular error is 2 mrad, the range error is 10 m. The plant noise parameter, ϵ, for the linear filter is 5g's. The plant noise parameter, η, for both of the extended filters is 0.1g's. The plant noise parameter, κ, for the first extended filter is 56,250 kg/m^2. The plant noise for the second extended filter is 5.6250x10^{-10} m^2/kg.

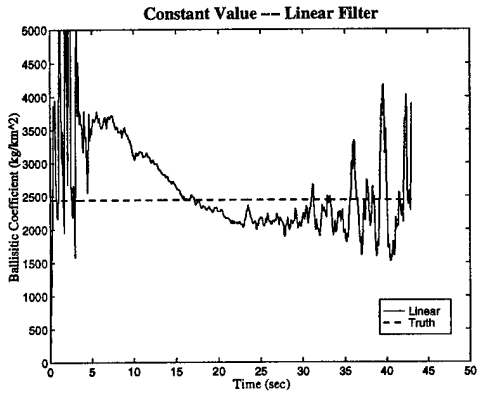

Figure 4: Estimation of β For Constant Profile

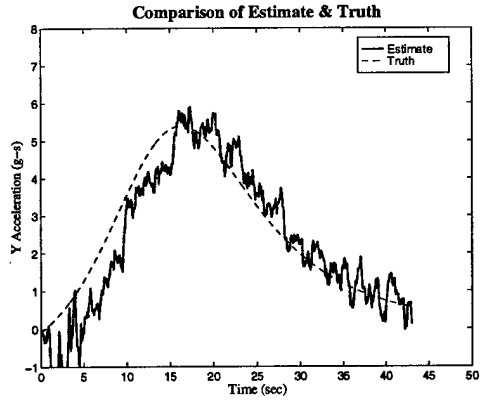

Figure 5: Linear filter estimation of the object's acceleraion in the Y direction.

For the first set of simulation cases the ballistic coefficient is assumed to be constant. Figure 4 shows that, after an initial transient period, the linear Kalman filter is able to estimate the ballistic coefficient. However, the estimate is extremely noisy and it is certainly not clear that the linear filter is behaving as well as it could.

In principal the linear filter is only suppose to estimate position, velocity and acceleration of the target.

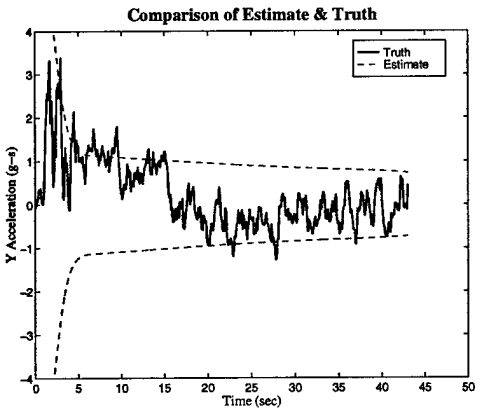

Figure 6: Predicted and actual error in the acceleration estimate in the Y direction for the Linear Filter.

In order to see if the linear filter was performing properly these estimates were examined in more detail. For example, Figure 5 indicates that the altitude portion of the acceleration is tracked extremely accurately (so is the downrange portion of acceleration). Although the estimate is somewhat noisy there is no apparent lag between the actual and estimated acceleration.

Figure 6 presents the error in the estimate of the altitude portion of target acceleration. Superimposed on the figure are the theoretical estimates, obtained from the Ricatti equations, of the error in the acceleration estimate. Since the single flight results are within the theoretical bounds approximately 68% of the time we can say that the filter is behaving correctly. In fact, we can see from Figure 6 that we can estimate target acceleration to within 1 g.

Why then is the linear filter estimate of the targets ballistic coefficient so bad when the acceleration estimates are so good? A careful examination of Eq. 22 from where the linear filter estimates the ballistic coefficient based on the state estimates reveals that there is a division by acceleration. Since the acceleration estimate is somewhat noisy (see Fig. 5), dividing by acceleration will multiply the noise and degrade the ballistic coefficient estimate.

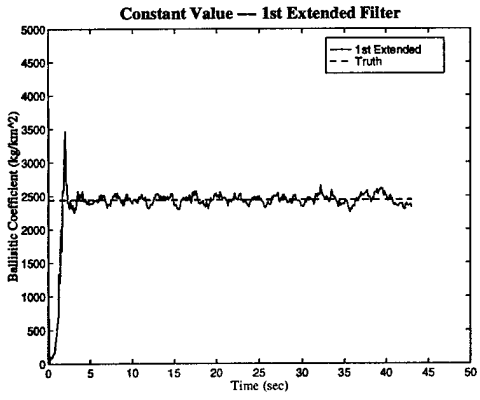

Figure 7: Estimation of β For Constant Profile

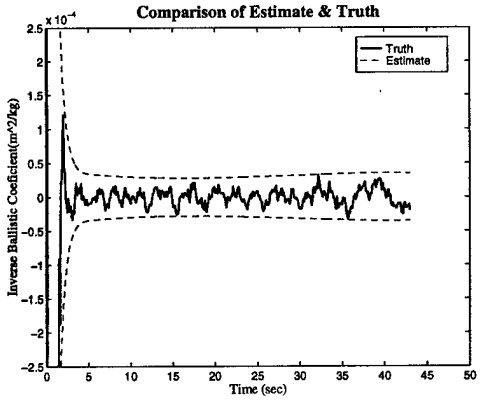

Figure 8: Predicted and actual error in the α estimate for the first extended filter.

Figure 7 shows that the first extended Kalman filter (with α as a state) does an excellent job of estimating the target's ballistic coefficient. After a brief transient period the estimate is virtually exact with only slight jitteriness. These estimates are superior to those of the linear filter. Figure 8 displays single flight results for the error in the estimate of α. Superimposed on the figure are the theoretical results from the Ricatti equations. Since the single flight results are within the theoretical bounds it appears that filter is behaving properly.

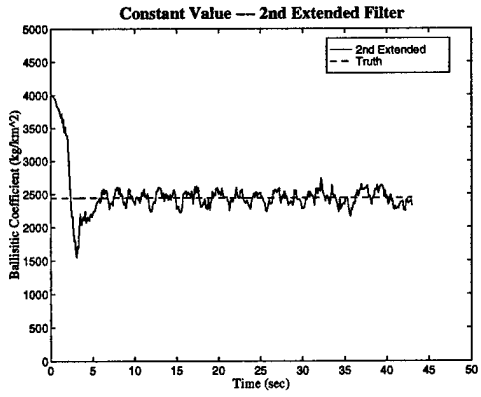

Figure 9: Estimation of β For Constant Profile

Figure 9 shows that the second extended Kalman filter (with β as a state) also does an excellent job of estimating the constant ballistic coefficient. These results are approximately the same as the first extended

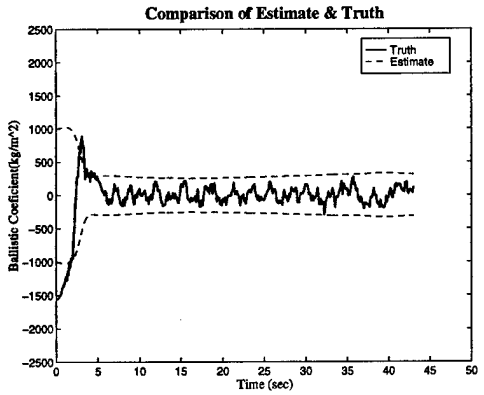

Figure 10: Predicted and actual error in the β estimate for the second extended filter.

Kalman filter and a great deal better than those of the linear Kalman filter. Figure 10 displays single flight results for the error in the estimate of β. Superimposed on the figure are the theoretical results from the Ricatti equations. Since the single flight results are within the theoretical bounds it appears that filter is behaving properly. We can also see that theory predicts that we should be able to estimate the ballistic coefficient to within 400 kg/m^2.

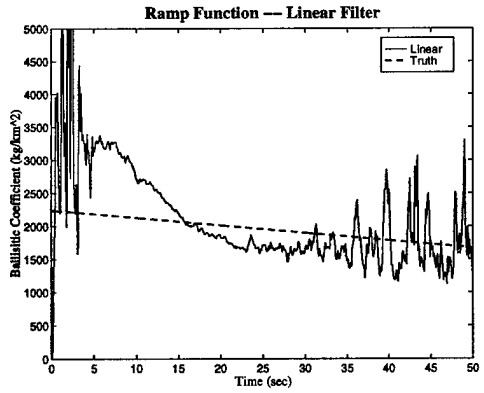

Figure 11: Estimation of β For A Ramped Profile

Next, the three filters were compared in terms of their ability to estimate the ballistic coefficient when the actual ballistic coefficient changed linearly with time. Figure 11 shows that the linear filter is able to estimate the time-varying ballistic coefficient but that it's estimates are still fairly noisy. Even though both extended Kalman filters did not assume the ballistic coefficient was time-varying they accounted for that possibility by including process noise on the ballistic coefficient state. Figures 12 and 13 indicate that the time-varying ballistic coefficient can be estimated quite well and that both extended Kalman filters are superior to the linear

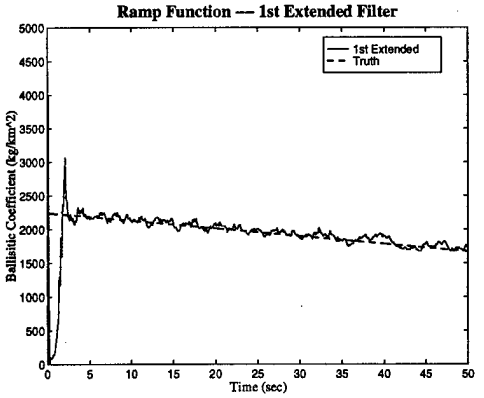

Figure 12: Estimation of β For A Ramped Profile

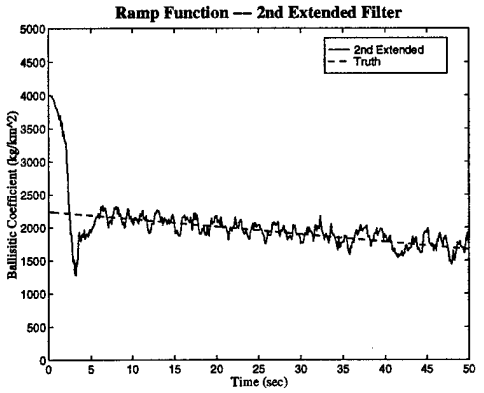

Figure 13: Estimation of β For A Ramped Profile

Kalman filter. However, the performance of both extended Kalman filters are approximately the same.

When a ballistic target reenters the atmosphere it can break up due to large loadings. If it breaks in half the ballistic coefficient will change by a factor of two. Therefore the filter's response to a step change in the target's ballistic coefficient can be important. Figure 14 shows that the linear filter is able to track the step change in the ballistic coefficient - but in it's usually noisy manner. Figures 15 and 16 show that both extended Kalman filters do an excellent job of tracking the step change. Both filters have a transient period initially and then, to a lesser degree, afterwards when the step change occurs. Again, the extended filter results are superior to the linear filter results and equivalent to each other.

If a radar can devote all its resources to tracking one object then high update rates (small Δt's) can be achieved. However, if many objects must be tracked then one may have to use a lower data rate (large Δt's). For this set of experiments it was assumed that the bal-

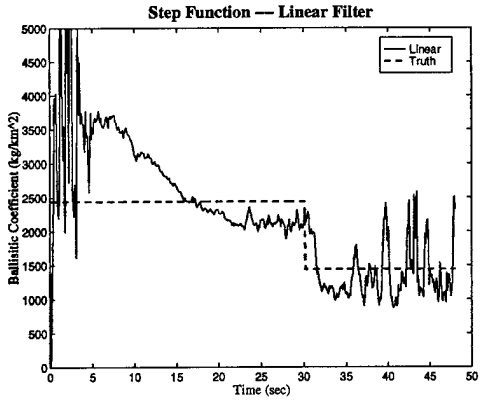

Figure 14: Estimation of β For A Profile With A Step

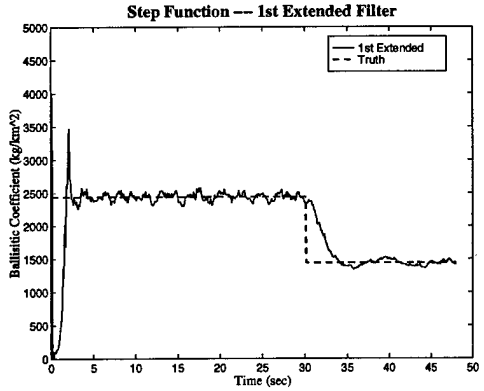

Figure 15: Estimation of β For A Profile With A Step

listic coefficient had a step change and that the filter sampling time increased from .1 s to 1 s. Figure 17 indicates that there is no degradation in the linear filter's ability to estimate the ballistic coefficient (compare to Fig. 14). In fact, the filter's estimates are less noisy because the sampling time is larger. The reason for the lack of filter degradation is that the fundamental matrix, used by the linear Kalman filter, is exact. Both extended Kalman filter's also have a good approximation to the fundamental matrix, (See Eq. 25), and Figs. 18 and 19 also show very little degradation in filter performance with the increase in the sampling time. Again we can say that both extended Kalman filters yield similar results and that both are superior to the linear Kalman filter.

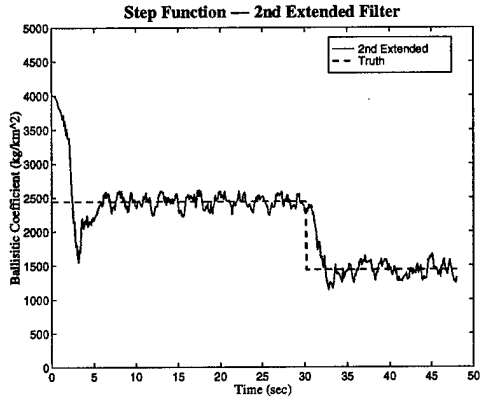

Figure 16: Estimation of β For A Profile With A Step

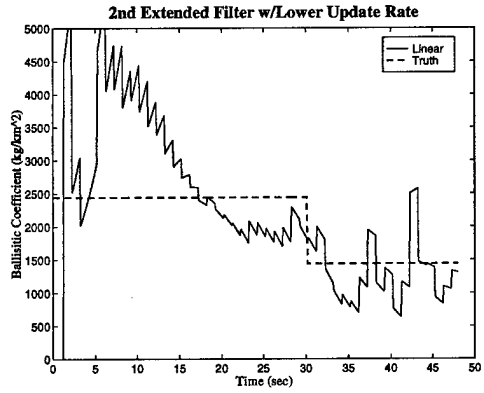

Figure 17: Estimation of β with a lower measurement rate.

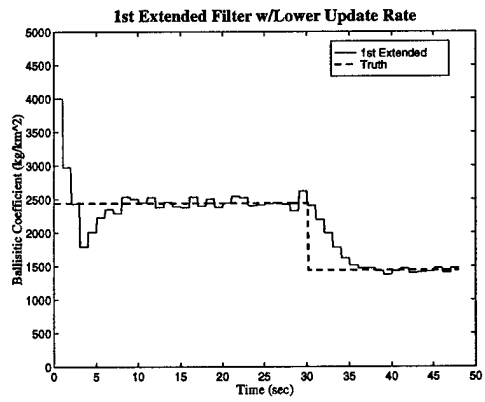

Figure 18: Estimation of β with a lower measurement rate.

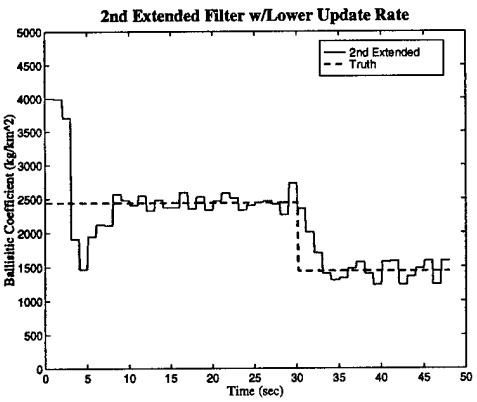

Figure 19: Estimation of β with a lower measurement rate.

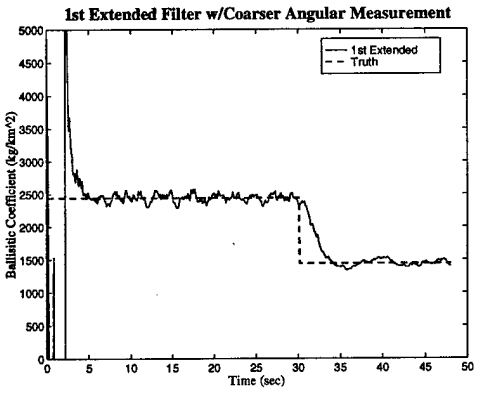

Figure 20: Estimation of β with a larger angular error.

At this point the linear Kalman filter is ruled out and for the final experiment we investigate how both extended Kalman filters perform when the measurement noise is made larger. For this example the measurement noise is increased from 2 mrad to 10 mrad. We can see from Figures 20 and 21 that the performance of both extended Kalman filters to a step change in the ballistic coefficient is excellent and not much different than when the measurement noise was smaller (see Figs. 15 and 16). Although there was more measurement noise in this case the filter performance was not noticably changed.

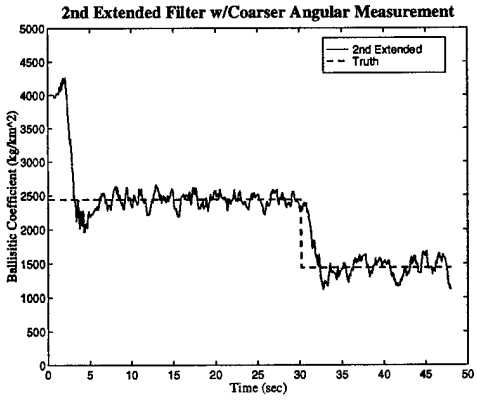

Figure 21: Estimation of β with a larger angular error.

Conclusions

A linear and two extended Kalman filters tracked an object as it reentered the atmosphere. Estimates of the ballistic coefficient were computed by all filters. The errors in these estimates were then computed and compared.

The performance of the linear filter was substantially poorer than that of the extended filter when estimating the ballistic coefficient of an endo-atmospheric trajectory. Both extended Kalaman Filters had similar performance so that one could conclude that the choice of state (β or α) was not important for this application. The choice of state did not impact the filter performance.

References

[1]Bryson, A. E. and Ho, Y., *Applied Optimal Control: Optimization, Estimation and Control*

[2]Bar-Shalom,Y. and Li, X., *Estimation and Tracking: Principals, Techniques and Software*, Artech house, London, 1993.

[3]Lawton, J. A., Jesionowski, R. J., Zarchan, P., "Comparison of Four Filtering Options For A Radar Tracking Problem" *Journal of Guidance, Control, and Dynamics Vol. 21, July-August 1998, pp618-623.*